



Published in final edited form as:

Biochemistry. 2010 February 16; 49(6): 1176–1182. doi:10.1021/bi901772w.

Reaction Coordinate of Isopenicillin N Synthase: Oxidase versus Oxygenase Activity

Christina D. Brown-Marshall, Adrienne R. Diebold, and Edward I. Solomon*

Department of Chemistry, Stanford University, Stanford, California 94305, USA

Abstract

Isopenicillin N synthase (IPNS) can have both oxidase and oxygenase activity depending on the substrate. For the native substrate, ACV, oxidase activity occurs; however for the substrate analogue ACOV, which lacks an amide nitrogen, IPNS shows oxygenase activity. The potential energy surfaces for the O-O bond elongation and cleavage were calculated for three different reactions: homolytic cleavage via traditional Fenton chemistry, heterolytic cleavage, and nucleophilic attack. These surfaces show that the hydroperoxide-Ferrous intermediate, formed by O₂ activated H atom abstraction from substrate, can undergo different reaction pathways and that interactions with the substrate govern the pathway. The hydroperoxide hydrogen bonds to the amide nitrogen of ACV polarizing the σ^* orbital of the peroxide toward the proximal oxygen, facilitating heterolytic cleavage. For the substrate analogue ACOV, this hydrogen bond is no longer present, leading to nucleophilic attack on the substrate intermediate C-S bond. After cleavage of the hydroperoxide, the two reaction pathways proceed with minimal barriers to result in the closure of the β -lactam ring for the oxidase activity (ACV) or formation of the thiocarboxylate for oxygenase activity (ACOV).

Isopenicillin N-synthase is a mononuclear non-heme iron enzyme found in fungi and bacteria that catalyzes the formation of isopenicillin N, a bicyclic precursor to the β lactam antibiotics including the penicillins and cephalosporins. (1,2) IPNS binds a tripeptide substrate δ -(L- α -aminoadipoyl)-L-cysteinyl-D-valine (ACV) and performs a four electron oxidative double ring closure, fully reducing one equivalent of O₂ to H₂O and closing the β lactam and thiazolidine rings of isopenicillin N. (3-6) (Scheme 1) This oxidase reactivity is unusual as most non-heme iron enzymes catalyze oxygenation reactions. Previous studies of the IPNS-ACV {FeNO}⁷ complex revealed that a major factor contributing to the oxidase reactivity of IPNS is charge donation from the ACV thiolate ligand, which renders the formation of the Fe^{III}-superoxide complex energetically favorable and drives the reaction only at the Fe center. (7) This single center, one electron reaction allows IPNS to avoid the bridged binding of O₂ between the Fe^{II} and the substrate/cofactor required for its two electron reduction; a reaction generally invoked for the non-heme Fe enzymes, that leads to oxygen insertion. The thiolate coordination of the IPNS ACV substrate further activates the reactive Fe^{III}-superoxide complex of the enzyme through a configuration interaction with the bound superoxide π^* orbital which creates

* To whom correspondence should be addressed: edward.solomon@stanford.edu; phone: 650-723-4694; fax: 650-725-0259.

IPNS: Isopenicillin N synthase

ACV: δ -(L- α -aminoadipoyl)-L-cysteinyl-D-valine

ACOV: δ -(L- α -aminoadipoyl)-L-cysteinyl-D- α -hydroxyisovaleryl ester

The reorientation of the hydroperoxide was accomplished through contraction of the distance between the ACV amide nitrogen and cysteinyl carbon to a distance of approximately 2.8Å.

Supporting Information Available: Full reference for reference 20; alleviation of backbonding with O-O bond elongation; bond lengths and spin densities for elongation of the O-O bond; Cartesian coordinates for selected structures. This material is available free of charge via the Internet at <http://pubs.acs.org>.

a Frontier Molecular Orbital (FMO) with correct orientation for H-atom abstraction from the ACV substrate. (7)

Density Functional Theory (DFT) studies of the reaction coordinate of IPNS reveal that the Fe^{III}-superoxide FMO will carry out the H-atom abstraction from the cysteinyl β carbon of ACV with a low barrier. H-atom abstraction from ACV is accompanied by an additional electron transfer from the ACV substrate to yield an Fe^{II}-hydroperoxide and a double bond between the thiol sulfur and adjacent carbon of ACV. (Box in Scheme 2) (8-11) This IPNS-Fe^{II}-hydroperoxide is proposed to deprotonate either the amide nitrogen of ACV (10,11) or the iron-bound water (9) and cleave the O-O bond heterolytically, resulting in the formation of H₂O and an Fe^{IV}-oxo species. An S_N2-type reaction occurs between the lone pair on the ACV amide nitrogen and the carbon of the C-S double bond, leading to ring closure and formation of the beta-lactam ring of isopenicillin N. (Center reaction, Scheme 1)

The heterolytic cleavage of the O-O bond of an Fe^{II}-hydroperoxide is unusual, as Fe^{II}-hydroperoxide is generally thought to undergo Fenton chemistry to cleave the O-O bond homolytically, resulting in the production of a hydroxyl radical and an Fe^{III}-oxo(OH⁻) species. (12-14) Baldwin et. al. have studied a series of ACV substrate analogues and have proposed mechanisms for their reactivity with dioxygen based upon crystal structures of the product complexes of these IPNS-Fe^{II}-analogue complexes after exposure to dioxygen. (15-19) In one such analogue ACOV, the amide nitrogen of the ACV valine is replaced with an oxygen atom as an ester, removing one of the proposed sources of the proton that could assist in O-O bond cleavage. Upon exposure to dioxygen, this analogue results in the hydroxylation of the cysteine carbon, effectively modifying the reactivity of IPNS from an oxidase to an oxygenase through a proposed nucleophilic attack of the Fe^{II}-hydroperoxide. (19) In this study, DFT calculations calibrated by our experimental studies of the IPNS-ACV-{FeNO}⁷ complex (7) were performed to explore how substrate interactions with the Fe^{II}-hydroperoxide moiety can avoid Fenton chemistry (homolytic cleavage) and modify the reactivity of this species, from heterolytic O-O bond cleavage to nucleophilic attack (Scheme 1). The exploration of factors governing reactivity (substrate direction of oxidase vs. oxygenase activity) adds a new facet of understanding to the body of knowledge on this important enzyme that has not been addressed in previous theoretical studies.

Methods

The starting geometry for the Fe-IPNS-ACV-O₂ complex was taken from the crystal structure of Fe-IPNS-ACV-NO from *Aspergillus nidulans*. (11) Protein-derived ligands were truncated with methyl imidizoles modeling histidines and propionate modeling aspartate. The ACV substrate was truncated to remove the 6 carbon aminoadipoyl chain but was otherwise left intact. The β -carbons of the protein ligands were frozen relative to each other to impose the constraints of the protein backbone. The cysteine nitrogen was also frozen relative to the alpha-carbons of the protein ligands to mimic hydrogen bonding to the substrate in the protein pocket.

All complexes were geometry optimized using the Gaussian 03 software package (20), with the spin unrestricted BP86 functional (21,22) with 10% Hartree-Fock exchange under tight convergence criteria. This functional was previously calibrated for mononuclear non-heme iron {FeNO}⁷ complexes. (23) Geometry optimizations were carried out using the Pople 6-311G* basis set on Fe, S, and the O₂ unit with the 6-31G* basis set on the remaining atoms. Single point calculations were performed on the optimized structures to generate molecular orbitals using the functional and basis set above. Orbital compositions were calculated using QMForge (24) and optimized structures and molecular orbitals were visualized using Molden version 4.1. (25) Frequencies and thermodynamic parameters were calculated using the split 6-311G*/6-31G* basis set. In order best describe the effects of the ACV sulfur interaction with

the Fe-IPNS models, single point energies were calculated for the Fe-IPNS-ACV complexes using the 6-311+G(2d,p) basis set. Solvation effects on the energy of the optimized structure were included using the Polarized Continuum Model (PCM) (26) with a dielectric constant $\epsilon = 4.0$ to model the protein environment. Cartesian coordinates for all models are given in the supplementary information.

Results

The Potential Energy Surfaces (PES) for homolytic O-O bond cleavage, heterolytic O-O bond cleavage and nucleophilic attack of three models of the IPNS active site were obtained as follows. The starting geometry for the Fe-IPNS-HO₂ complexes was taken from previously optimized Fe-IPNS-ACV-O₂ structure (7) with subsequent ACV H-atom abstraction. After H-atom abstraction from the ACV carbon, the Fe^{II}-IPNS-ACV-HO₂ complex relaxes through reorientation of the hydroperoxide moiety to optimize hydrogen bonding interactions with the ACV amide and carboxylate residues (Figure 1, Model 1).² In order to model the nucleophilic attack by hydroperoxide seen for the ACOV substrate, the IPNS-Fe-ACV-HO₂ was truncated between the α -carbon and carbonyl carbon of the cysteine (Figure 1, Model 2), thus removing the amide nitrogen. Finally, this truncated ACOV model was used to explore the homolytic cleavage reaction by introducing a constraint on the model to fix the distance between the distal peroxide oxygen atom and the carbon atom of the substrate, preventing the interaction of the distal oxygen with the ACOV carbon (Figure 1, Model 3).

For all three models studied, the electronic structure of the starting Fe^{II}-hydroperoxide complex is similar and is shown in Figure 2. Both the in-plane (ip) and out-of-plane (op) $2\pi^*$ orbitals of the hydroperoxide are fully occupied and the unoccupied σ^* orbital of the hydroperoxide has come down in energy, in preparation for O-O bond cleavage. (27) As previously described, (9) the Fe d_{xy} orbital in the β manifold is occupied, and a double bond has formed between the cysteine carbon and sulfur atoms, evidenced by the unoccupied C-S π^* orbital in both the α and β manifolds. At the optimized O-O bond length, there is a mixing of the occupied β Fe d_{xy} orbital and the C-S π^* orbital, which is indicative of backbonding of the occupied Fe^{II} d orbital into the C-S π^* double bond. As the O-O bond is elongated, this backbonding is alleviated, localizing the electron on the Fe and allowing the occupied β Fe d_{xy} orbital to rotate to interact with the descending hydroperoxide σ^* orbital. (Figure S1)

Starting with the optimized Fe^{II}-hydroperoxide structures, the PES of each model was explored by optimizing each structure with incrementally increasing O-O bond distance until the O-O bond was fully cleaved. Optimized geometries for the O-O elongation along the PES's of **1**, **2** and **3** are shown in Figure 3 and key computational results are summarized in Table S1. The PES of **3** corresponds to the expected Fenton chemistry with homolytic cleavage of the O-O bond. This homolytic cleavage is accomplished by transfer of one β electron from the Fe d_{xy} orbital to the O-O σ^* orbital (Figure 4, left), resulting in the formation of an Fe^{III}-oxo complex and a hydroxyl radical. This is evidenced by the accumulation of negative spin density on the distal oxygen (-0.48 at O-O 2.20Å. See Table S1). The PES of **1** (Figure 3, middle) proceeds as a heterolytic cleavage of the O-O bond, with one electron in each spin manifold transferred from the β Fe d_{xy} orbital and the α Fe d_{z^2} into the O-O σ^* orbital (Figure 4, middle). This produces an Fe^{IV}-oxo complex and hydroxide, which remains within hydrogen-bonding distance of the amide of the ACV valine (Figure 3, middle right). The PES of model **2** involves a nucleophilic attack of the hydroperoxide moiety at the ACOV carbon followed by heterolytic O-O bond cleavage (Figure 3, bottom). Nucleophilic attack is accomplished by the transfer of an electron pair from the peroxide π^* out-of-plane orbital to the C-S π^* orbital (Figure 4, right), followed by two electron transfer from the Fe^{II} to the O-O σ^* orbital to give an Fe^{IV}-oxo complex with a hydroxylated substrate carbon.

These calculated model reactions demonstrate that the same Fe^{II}-hydroperoxide unit can undergo different reaction modes. The factors that govern the choice of reaction pathways were evaluated further. Table S1 shows that at short distances, models 1 (heterolytic) and 3 (homolytic) show similar electronic structure up to 1.9 Å for the transfer of the first electron from Fe^{II} to the hydroperoxide σ^* orbital. A plot of the energies along the reaction coordinate for models 1 (heterolytic) and 3 (homolytic) (Figure 5) shows an initial stabilization of this electron transfer, and this stabilization is expected to be similar for the second electron in the heterolytic O-O bond cleavage pathway as opposed to the homolytic pathway. Comparing the structures, the distal oxygen of the heterolytically cleaving **1** is within hydrogen bonding distance of the amide proton of the ACV valine, while the distal oxygen of the homolytic coordinate **3** has no such interaction. This hydrogen bond in **1** stabilizes the transfer of both electrons to the distal oxygen.

Importantly, **1** has an unoccupied σ^* orbital that is polarized toward the proximal oxygen (Op, Figure 6, left), while the σ^* orbital of **3** is polarized toward the distal oxygen (Od, Figure 6, middle). When the σ^* orbital is polarized toward the proximal oxygen, its bonding σ counterpart is polarized toward the distal oxygen. As this peroxide σ orbital is fully occupied, this polarization will lead to an electron pair being transferred to the distal oxygen upon O-O bond cleavage thus the heterolytic cleavage of the O-O bond. Polarization of the σ^* orbital toward the distal oxygen allows only for the transfer of a single electron to the distal oxygen and results in homolytic cleavage. The hydrogen bonding interaction of **1** can be modeled by adding an equivalent point dipole to **3**, which reverses the polarization of the σ^* orbital (Figure 6, right). Elongation of the O-O bond in the presence of a point dipole also leads to heterolytic cleavage (Table S2). Therefore, it is the interaction of the dipole of the amide N-H bond with the distal oxygen in **1** that directs the ACV complex toward heterolytic cleavage of the O-O bond.

In comparing the nucleophilic attack relative to the heterolytic O-O bond cleavage (**2** vs. **1**), both of these pathways proceed with similarly small reaction barriers (Figure 5). From a more detailed transition state analysis on model 1, the ΔG^\ddagger is 4.1 kcal/mol. (The coordinates are given in Table S5; the transition state occurs at an O-O bond length of approximately 1.6 Å.) In order for **1** to undergo a nucleophilic attack, the hydrogen bond between the distal oxygen and the amide proton would have to be broken to allow the peroxide to rotate to the proper orientation (Scheme 3).

The strength of the hydrogen bonding interaction that must be broken in order for the hydroperoxide to undergo this rotation is calculated to be 5.6 kcal/mol, which is already larger than the barrier for heterolytic cleavage (Figure 5). This hydrogen bonding interaction with the amide proton in **1** would thus bias the reaction of the Fe^{II}-hydroperoxide toward heterolytic cleavage over nucleophilic attack. In this way, the hydrogen bonding interaction of the Fe^{II}-hydroperoxide helps distinguish between reactions possible for the IPNS- Fe^{II}-hydroperoxide-ACV intermediate. As the iron-bound water (the alternate proposed source for the proton in the reaction with ACV (9)) would be present in both the IPNS- Fe^{II}-hydroperoxide-ACV and IPNS-Fe^{II}-hydroperoxide-ACOV complexes, hydrogen bonding to the water would direct both complexes toward heterolytic cleavage of the O-O bond. Thus the observed nucleophilic reactivity of the ACOV complex argues strongly against the coordinated water being the source of the proton in either reaction.

The coordinates were extended beyond O-O bond cleavage to complete the reaction cycle for the different substrates. For **1**, the hydroxide produced upon O-O bond cleavage is within hydrogen-bonding distance of the amide proton of the ACV valine and can abstract this proton with a negligible barrier (< 1 kcal/mol) compared to the previous intermediate. This leaves a lone pair of electrons on the valine amide with appropriate overlap for a S_N2-type reaction with

the C-S π^* orbital to close the β -lactam ring of isopenicillin N (Figure 7). The orientation of the lone pair on the ACV amide is mechanistically significant, thus the ACV amide must be deprotonated before β -lactam ring closure. This reaction pathway is similar to that of the previous literature. (10) For **2**, the transfer of two protons, one from the hydroxyl group and one from the hydroxylated carbon of ACOV to the Fe-oxo would lead to the Fe-IPNS-Thiocarboxylate structure observed (19) for the oxygen-exposed Fe-IPNS-ACOV complex (Scheme 2, bottom).

Discussion

In the first stage of the reaction of the IPNS- Fe^{II}-ACV complex with dioxygen, the ACV thiolate bond activates the one electron reduction of dioxygen to form an Fe^{III}-superoxide complex with good FMO overlap for H-atom abstraction from the substrate.(7) This is atypical for most mononuclear non-heme Fe enzymes as seen in, for example, the α -ketoglutarate dependent and extradiol dioxygenases where the unfavorable one electron reduction of O₂ is circumvented by adopting a bridged binding mode allowing 2e⁻ reduction that results in oxygenase activity. This mechanism of a one e⁻ reduction of O₂ avoids its bridged binding to substrate and opens up a pathway for oxidase activity in IPNS not energetically available for other mononuclear non-heme Fe enzymes.

The initial H-atom abstraction in IPNS is calculated to produce an Fe^{II}-hydroperoxide complex that can undergo a variety of reaction channels, dependent upon its interaction with the substrate. While Fe^{II}-hydroperoxide species are generally thought to undergo Fenton chemistry (i.e. homolytic O-O bond cleavage in solution), the experimental evidence from reactions of IPNS-Fe^{II}-ACV and analogue complexes suggests that an Fe^{II}-hydroperoxide can follow alternative reaction pathways including heterolytic O-O bond cleavage and nucleophilic attack by the peroxide at a substrate double bond. DFT calculations on three IPNS-Fe^{II}-HO₂ models show that all three of the above reaction pathways are energetically accessible.

A fourth reaction pathway, not invoked in previous IPNS mechanisms but proposed for hydroxyethylphosphonate dioxygenase (HEPD), involves attack via the proximal oxygen of the hydroperoxide (with respect to the Fe center). This reaction is different from HEPD in that, for IPNS, it would involve the nucleophilic attack by the hydroperoxide but in HEPD, a hydroperoxylation is invoked.(28) To evaluate this pathway, the C...O_p reaction coordinate was examined. Starting from the optimized Fe^{II}-hydroperoxide structure (Figure 1, model **2**), the attack by the proximal oxygen occurs with a barrier of 2-3 kcal/mol, comparable to that observed in Figure 4 for the nucleophilic attack by the distal oxygen. Upon formation of the C-O_p bond, the C-S thioaldehyde is reduced while the Fe center remains Fe^{II} (Scheme 4, bottom). This intermediate is lower in energy than the starting structure by ~21 kcal/mol (compared to -67 kcal/mol for the Fe^{IV}-oxo intermediate from the nucleophilic attack by the distal oxygen, Scheme 4, top). From this intermediate, the O-O bond can be cleaved heterolytically and a proton lost from the C center to give the crystallographically observed thiocarboxylate intermediate. Although along a different reaction coordinate and with less driving force, attack by the proximal oxygen appears to be an additional, viable pathway that will lead to the product observed in the crystallography.

The DFT calculations show that the substrate interactions with the Fe^{II}-hydroperoxide moiety can determine its reactivity. For the ACV substrate, hydrogen bonding interactions with the amide hydrogen polarize the peroxide σ^* orbital to make the heterolytic cleavage of the O-O bond energetically favorable. In the absence of this hydrogen bonding interaction, nucleophilic attack of either the distal or proximal O of the hydroperoxide at the carbon of the ACV C-S double bond occurs, leading to the substrate hydroxylation observed experimentally for ACOV.

In this way the hydrogen bonding interaction with the ACV substrate directs the Fe^{II}-hydroperoxide to heterolytic cleavage and enables the unusual oxidase activity of this enzyme.

Supplementary Material

Refer to Web version on PubMed Central for supplementary material.

Acknowledgments

We thank Dr. Marcus Lundberg for insightful discussions.

This research was supported by NIH Grant GM40392.

References

1. Baldwin JE, Adlington RM, Moroney SE, Field LD, Ting HH. Stepwise Ring-Closure in Penicillin Biosynthesis - Initial Beta-Lactam Formation. *J Chem Soc Chem Commun* 1984:984–986.
2. Baldwin JE, Abraham E. The Biosynthesis of Penicillins and Cephalosporins. *Nat Prod Rep* 1988;5:129–145. [PubMed: 3145474]
3. Chen P, Solomon EI. Oxygen activation by the noncoupled binuclear copper site in peptidylglycine alpha-hydroxylating monooxygenase. Reaction mechanism and role of the noncoupled nature of the active site. *J Am Chem Soc* 2004;126:4991–5000. [PubMed: 15080705]
4. Orville AM, Chen VJ, Kriauciunas A, Harpel MR, Fox BG, Munck E, Lipscomb JD. Thiolate Ligation of the Active-Site Fe²⁺ of Isopenicillin-N Synthase Derives from Substrate Rather Than Endogenous Cysteine - Spectroscopic Studies of Site-Specific Cys -] Ser Mutated Enzymes. *Biochemistry* 1992;31:4602–4612. [PubMed: 1316153]
5. Randall CR, Zang Y, True AE, Que L, Charnock JM, Garner CD, Fujishima Y, Schofield CJ, Baldwin JE. X-Ray-Absorption Studies of the Ferrous Active-Site of Isopenicillin N-Synthase and Related Model Complexes. *Biochemistry* 1993;32:6664–6673. [PubMed: 8329393]
6. Scott RA, Wang SK, Eidsness MK, Kriauciunas A, Frolik CA, Chen VJ. X-Ray Absorption Spectroscopic Studies of the High-Spin Iron(II) Active-Site of Isopenicillin-N Synthase - Evidence for Fe-S Interaction in the Enzyme Substrate Complex. *Biochemistry* 1992;31:4596–4601. [PubMed: 1581312]
7. Brown CD, Neidig ML, Neibergall MB, Lipscomb JD, Solomon EI. VTVH-MCD and DFT studies of thiolate bonding to {FeNO}(7)/{FeO₂}(8) complexes of isopenicillin N synthase: Substrate determination of oxidase versus oxygenase activity in nonheme Fe enzymes. *J Am Chem Soc* 2007;129:7427–7438. [PubMed: 17506560]
8. Lundberg M, Morokuma K. Protein environment facilitates O₂ binding in non-heme iron enzyme. An insight from ONIOM calculations on isopenicillin N synthase (IPNS). *J Chem Phys B* 2007;111:9380–9389.
9. Lundberg M, Siegbahn PEM, Morokuma K. The mechanism for isopenicillin N synthase from density-functional modeling highlights the similarities with other enzymes in the 2-his-1-carboxylate family. *Biochemistry* 2008;47:1031–1042. [PubMed: 18163649]
10. Lundberg M, Kawatsu T, Vreven T, Frisch MJ, Morokuma K. Transition States in a Protein Environment - ONIOM QM:MM Modeling of Isopenicillin N Synthesis. *J Chem Theory Comput* 2009;5:222–234.
11. Roach PL, Clifton IJ, Hensgens CMH, Shibata N, Schofield CJ, Hajdu J, Baldwin JE. Structure of isopenicillin N synthase complexed with substrate and the mechanism of penicillin formation. *Nature* 1997;387:827–830. [PubMed: 9194566]
12. Haber F, W J. The Catalytic Decomposition of Hydrogen Peroxide by Iron Salts. *Proc R Soc Lond A* 1934;147:332–351.
13. MacFaul PA, Wayner DDM, Ingold KU. A radical account of “oxygenated Fenton chemistry”. *Acc Chem Res* 1998;31:159–162.
14. Walling C. Fentons Reagent Revisited. *Acc Chem Res* 1975;8:125–131.

15. Ge W, Clifton IJ, Stok JE, Adlington RM, Baldwin JE, Rutledge PJ. Isopenicillin N synthase mediates thiolate oxidation to sulfenate in a depsipeptide substrate analogue: Implications for oxygen binding and a link to nitrile hydratase? *J Am Chem Soc* 2008;130:10096–10102. [PubMed: 18620394]
16. Long AJ, Clifton IJ, Roach PL, Baldwin JE, Schofield CJ, Rutledge PJ. Structural studies on the reaction of isopenicillin N synthase with the substrate analogue delta-(L-alpha-aminoadipoyl)-L-cysteiny-D-alpha-aminobutyrate. *Biochem J* 2003;372:687–693. [PubMed: 12622704]
17. Long AJ, Clifton IJ, Roach PL, Baldwin JE, Rutledge PJ, Schofield CJ. Structural studies on the reaction of isopenicillin N synthase with the truncated substrate analogues delta-(L-alpha-aminoadipoyl)-L-cysteiny-glycine and delta-(L-alpha-aminoadipoyl)-L-cysteiny-D-alanine. *Biochemistry* 2005;44:6619–6628. [PubMed: 15850395]
18. Howard-Jones AR, Rutledge PJ, Clifton IJ, Adlington RM, Baldwin JE. Unique binding of a non-natural L,L,L-substrate by isopenicillin N synthase. *Biochem Biophys Res Commun* 2005;336:702–708. [PubMed: 16143309]
19. Ogle JM, Clifton IJ, Rutledge PJ, Elkins JM, Burzlaff NI, Adlington RM, Roach PL, Baldwin JE. Alternative oxidation by isopenicillin N synthase observed by X-ray diffraction. *Chem Biol* 2001;8:1231–1237. [PubMed: 11755401]
20. Frisch MJ, et al. Gaussian03, revision E.01. 2007
21. Perdew JP. Density-Functional Approximation for the Correlation-Energy of the Inhomogeneous Electron-Gas. *Physical Review B* 1986;33:8822–8824.
22. Becke AD. Density-Functional Exchange-Energy Approximation with Correct Asymptotic-Behavior. *Physical Review A* 1988;38:3098–3100. [PubMed: 9900728]
23. Schenk G, Pau MYM, Solomon EI. Comparison between the geometric and electronic structures and reactivities of {FeNO}(7) and {FeO2}(8) complexes: A density functional theory study. *J Am Chem Soc* 2004;126:505–515. [PubMed: 14719948]
24. Tenderholt AL. QMForge, Version 2.1.
25. Schaftenaar G, Noordik JH. Molden: a pre- and post-processing program for molecular and electronic structures. *J Comput-Aided Mol Des* 2000;14:123–134. [PubMed: 10721501]
26. Cramer CJ, Truhlar DG. Implicit solvation models: Equilibria, structure, spectra, and dynamics. *Chem Rev* 1999;99:2161–2200. [PubMed: 11849023]
27. Neese F, Zaleski JM, Zaleski KL, Solomon EI. Electronic structure of activated bleomycin: Oxygen intermediates in heme versus non-heme iron. *J Am Chem Soc* 2000;122:11703–11724.
28. Whitteck JT, Cicchillo RM, van der Donk WA. Hydroperoxylation by Hydroxyethylphosphonate Dioxygenase. *J Am Chem Soc* 2009;131:16225–16232. [PubMed: 19839620]

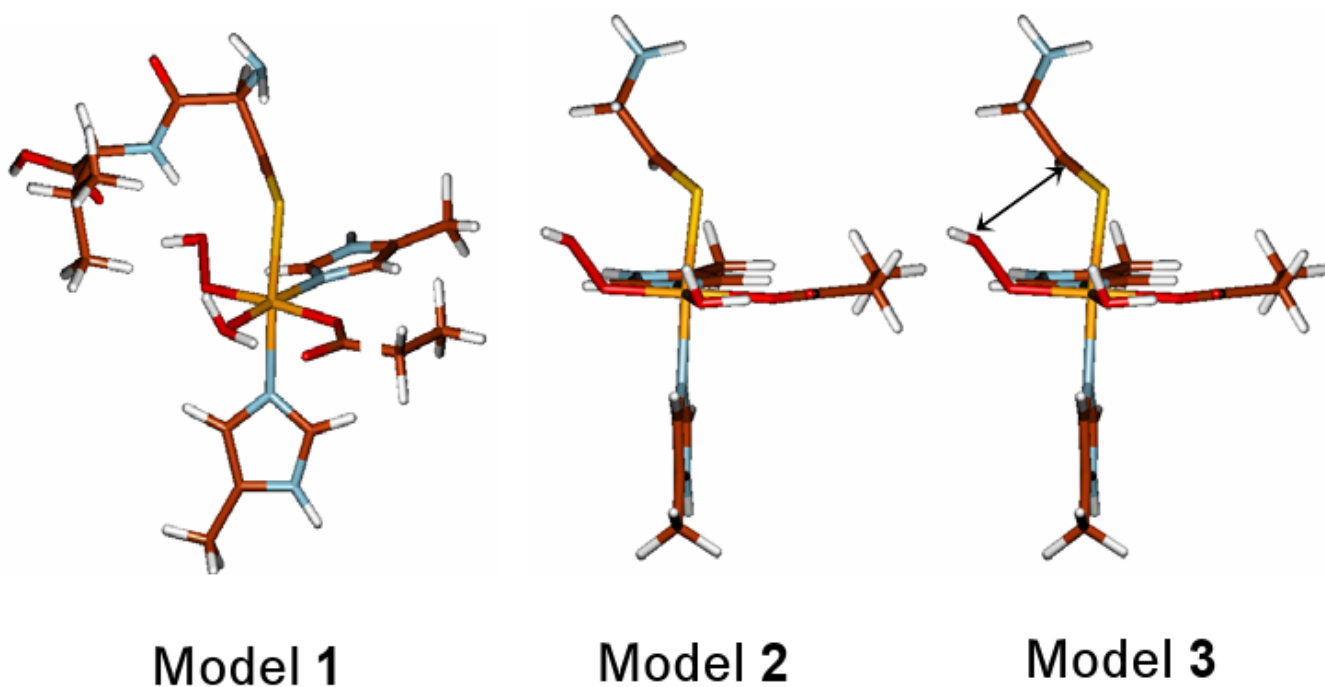


Figure 1. Models Used to Calculate Three Reaction Pathways of Fe^{II}-Hydroperoxide
The arrow in Model 3 indicates the extra constraint added to prohibit interaction of the distal oxygen with the carbon of the substrate.

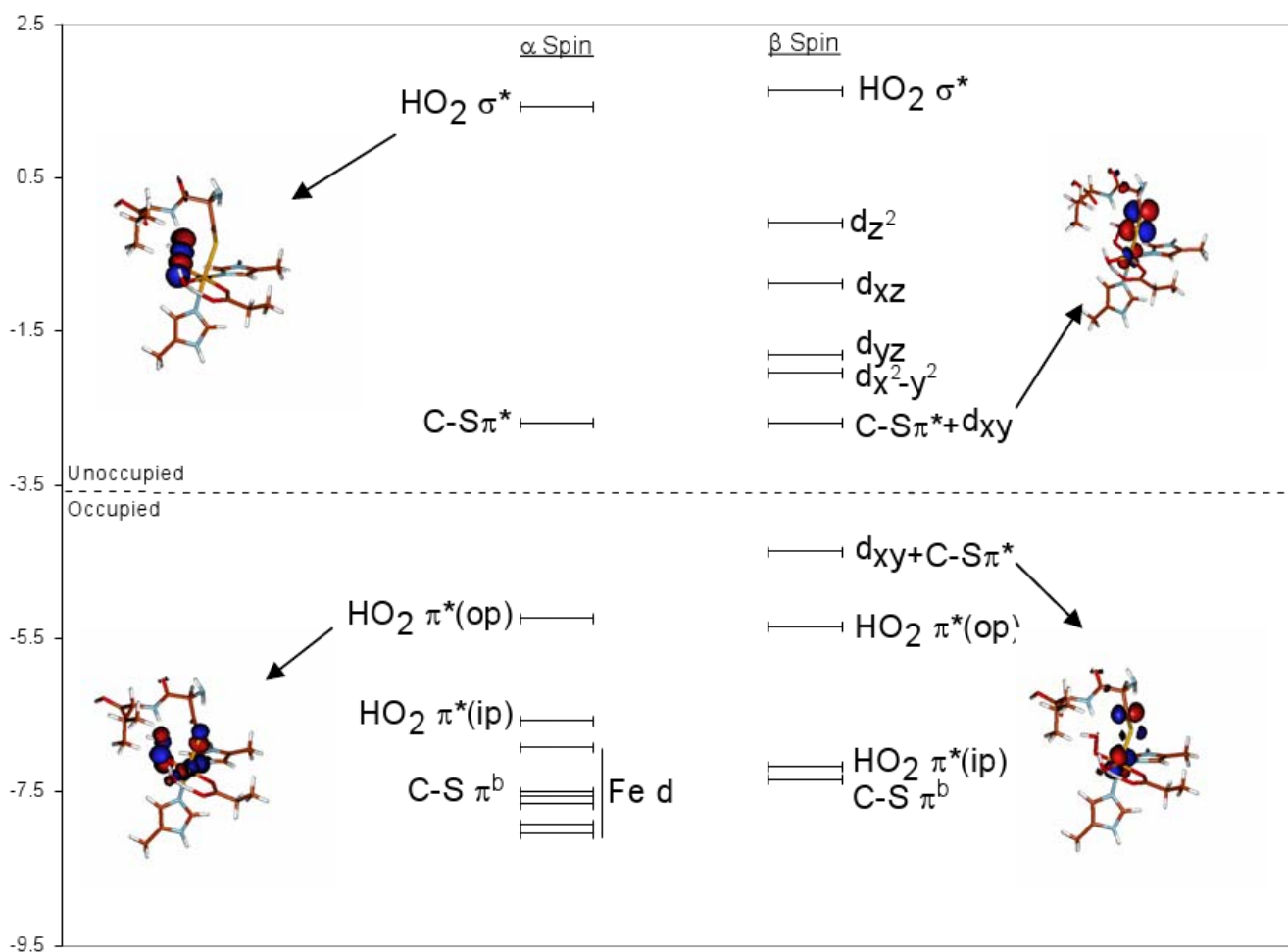


Figure 2. Molecular Orbital Diagram of IPNS-ACV-Fe^{II}-Hydroperoxide

Spin unrestricted contours given for representative molecular orbitals. Note the 4 unoccupied β d orbitals indicating Fe^{II}, and the unoccupied α , β pair of the σ^* orbital of peroxide with the α , β unoccupied pair of C-S π^* orbitals of the substrate π bond. The observed d_{xy} character (24%) in the C-S π^* bond reflects backbonding.

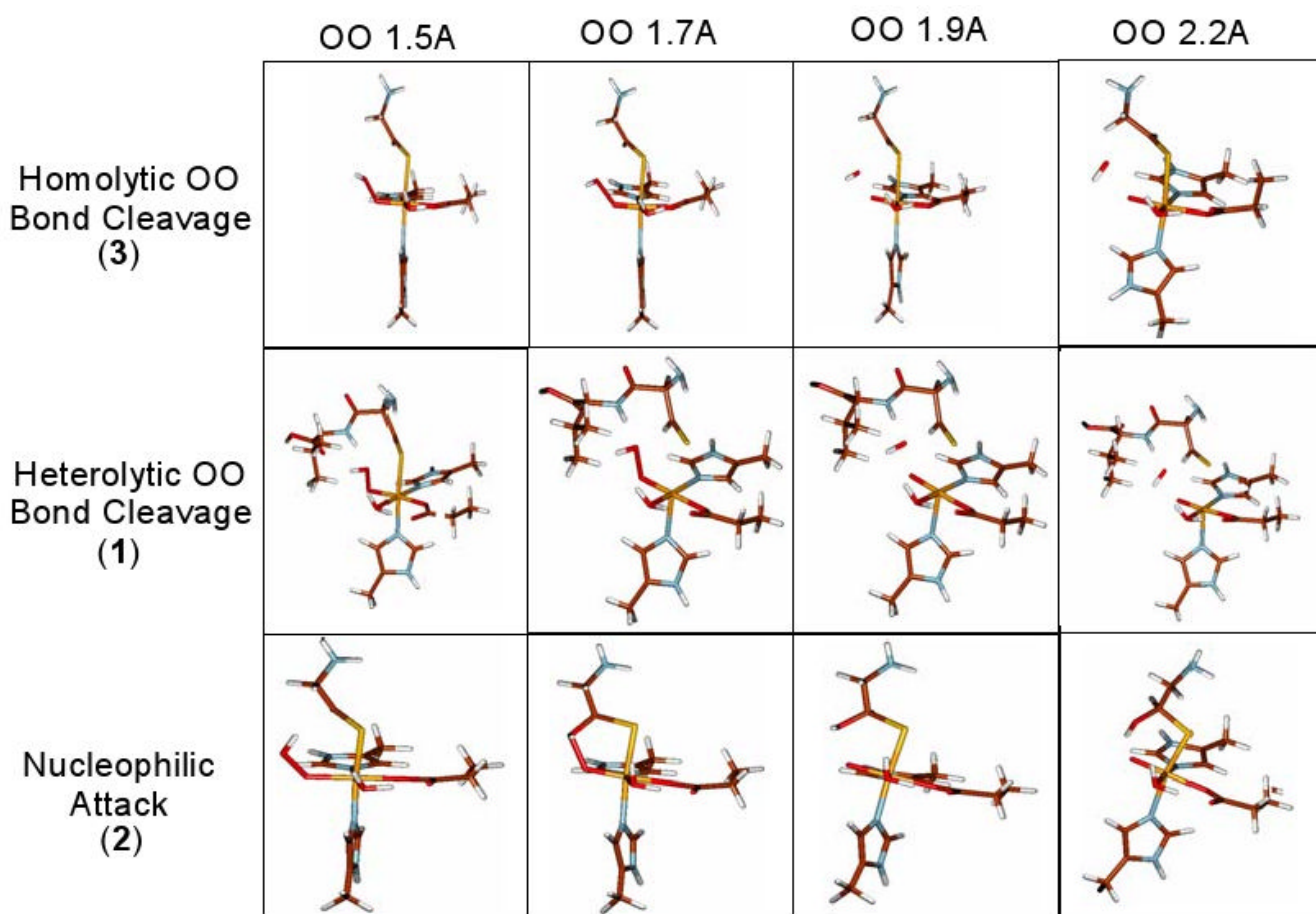
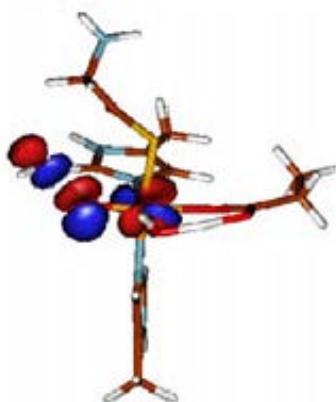


Figure 3. Geometric Structures of IPNS-Fe^{II}-Hydroperoxide Complexes with O-O Bond Elongation

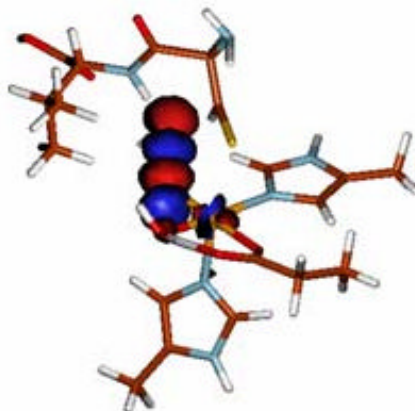
The three models undergo homolytic cleavage (top, 3), heterolytic O-O bond cleavage (middle, 1) and nucleophilic attack by the peroxide (bottom, 2).

Homolytic Cleavage (3)



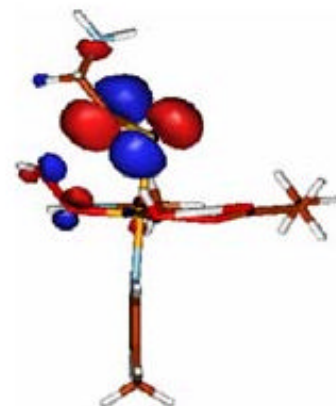
β Acceptor: $\text{HO}_2 \sigma^*$

Heterolytic Cleavage (1)

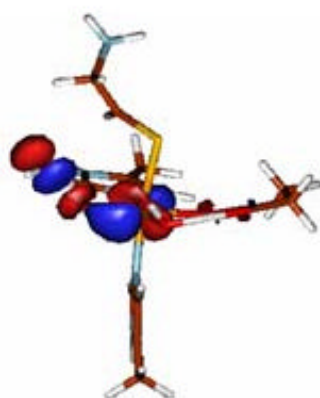


α Acceptor: $\text{HO}_2 \sigma^*$

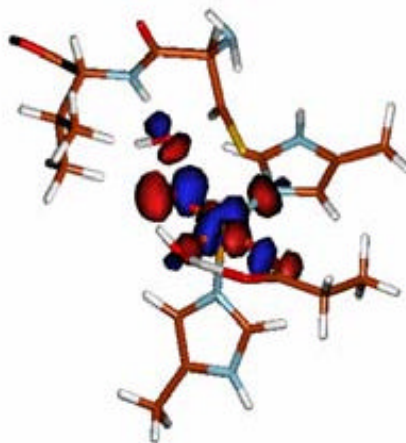
Nucleophilic Attack (2)



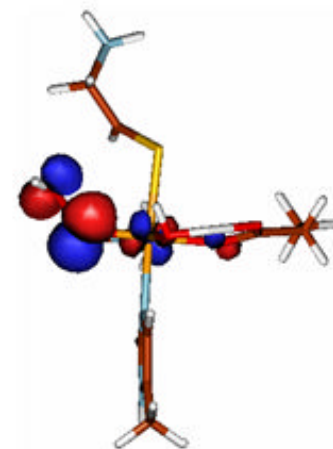
α Acceptor: $\text{C-S } \pi^*$



β Donor: $\text{Fe } d$



α Donor: $\text{Fe } d_z^2$



α Donor: $\text{HO}_2 \pi^*$

Figure 4. Donor and Acceptor Orbitals for Homolytic Cleavage, Heterolytic Cleavage and Nucleophilic Attack

In the homolytic cleavage reaction, one β electron is transferred from the $\text{Fe } d$ to the hydroperoxide σ^* orbital. Heterolytic cleavage and nucleophilic attack involve the transfer of an $\alpha\beta$ electron pair. For clarity, only the alpha donor and acceptor orbitals of these electron pairs are shown.

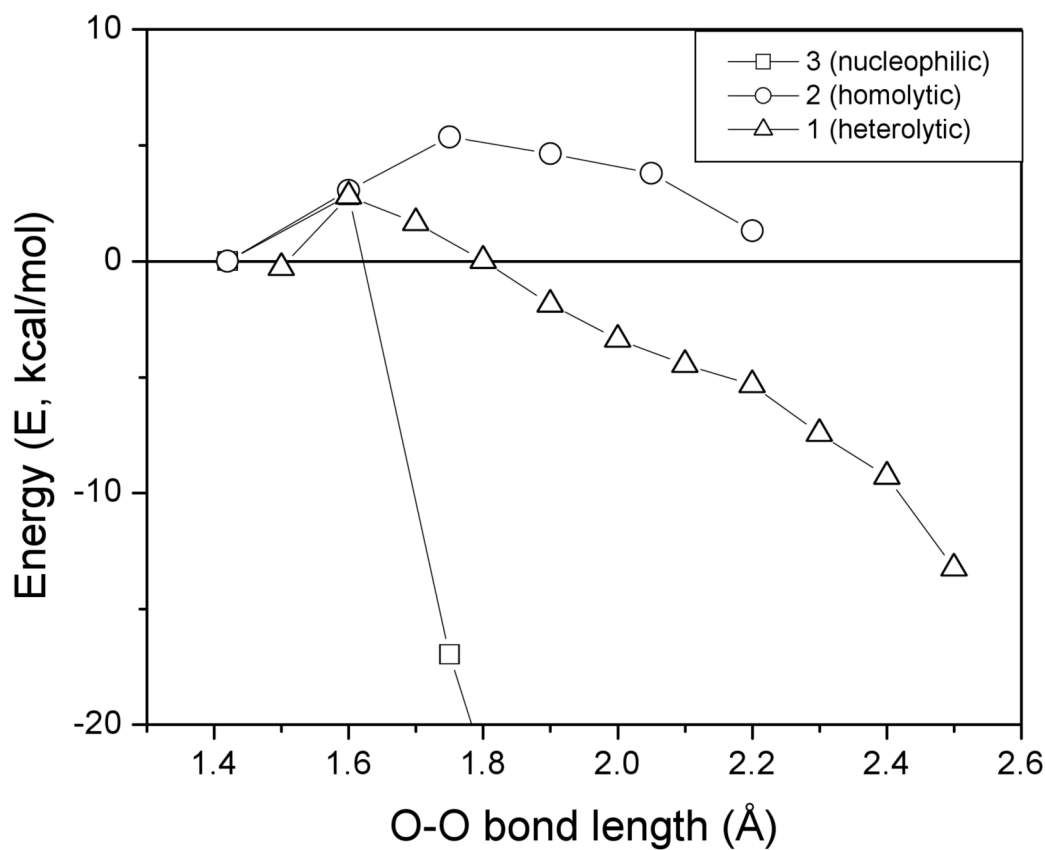


Figure 5. Energetics of O-O Bond Cleavage

The relative electronic energies are plotted for the homolytic cleavage (3, red circles), heterolytic cleavage (1, blue triangles) and nucleophilic attack (2, black squares) models as the O-O bond is elongated. Note that the nucleophilic attack model is only valid for O-O bond cleavage in ACOV and that for the ACV substrate, an additional barrier to break the amide-peroxide hydrogen bond is present.

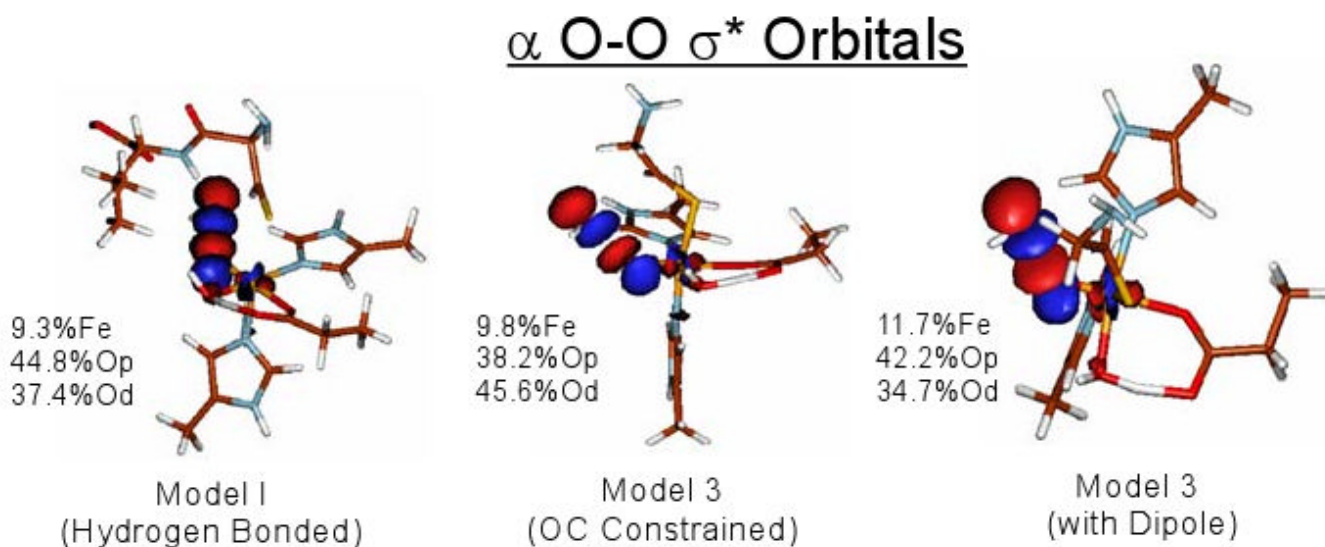


Figure 6. Alpha Hydroperoxide σ^* Orbitals

This orbital polarizes toward the proximal oxygen in Model 1, directing the reaction to heterolytic O-O bond cleavage, and toward the distal oxygen in Model 3, directing its reaction to homolytic O-O bond cleavage. By modeling the dipole interaction of the ACV amide N-H, the polarization of the σ^* bond in Model 3 is reversed

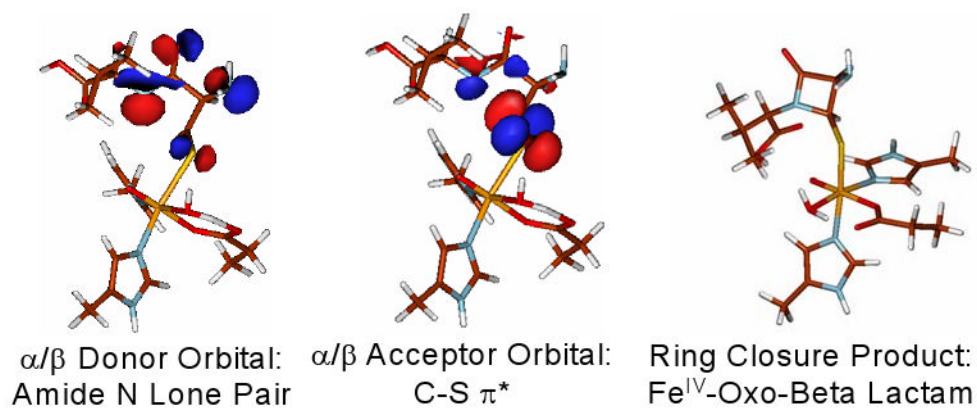
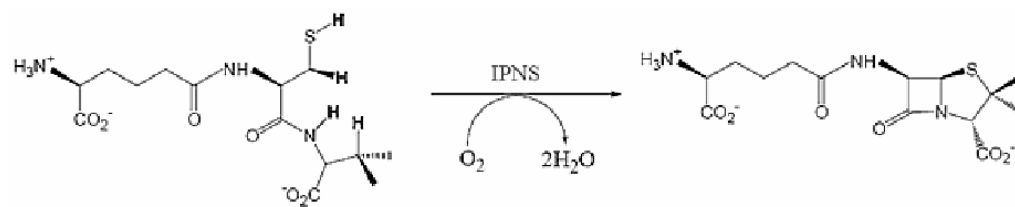
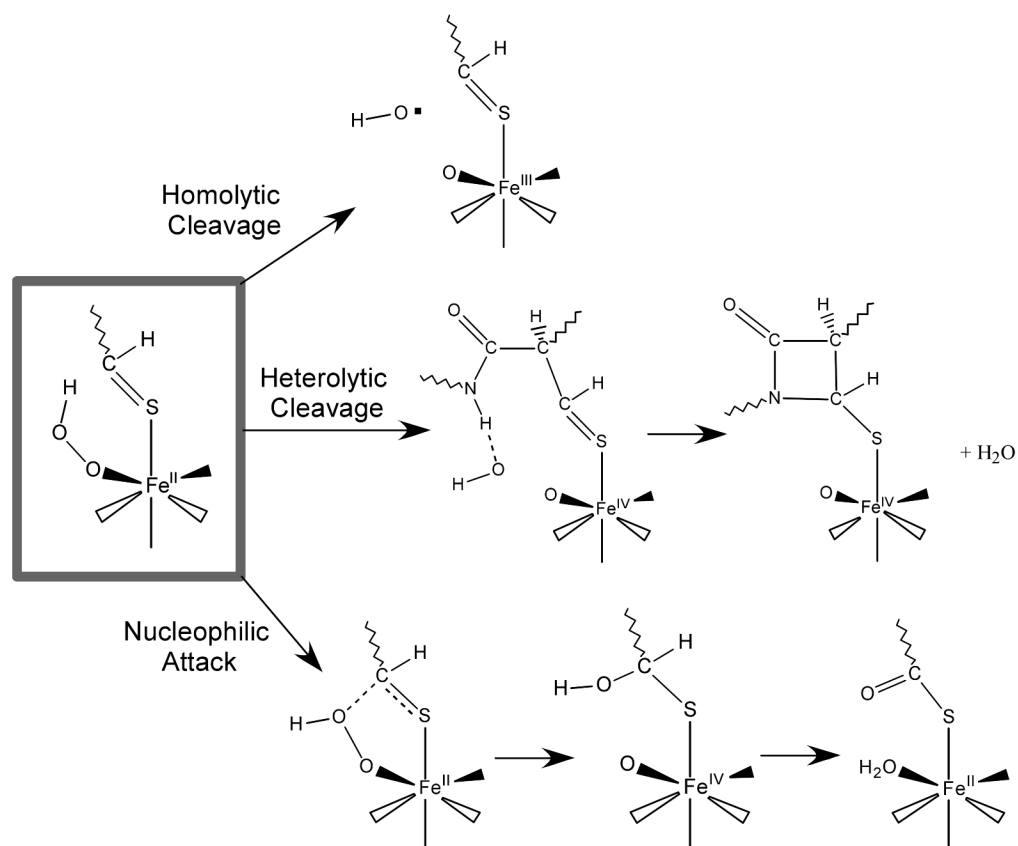


Figure 7. Donor and Acceptor Orbitals and Product for Beta-Lactam Ring Closure

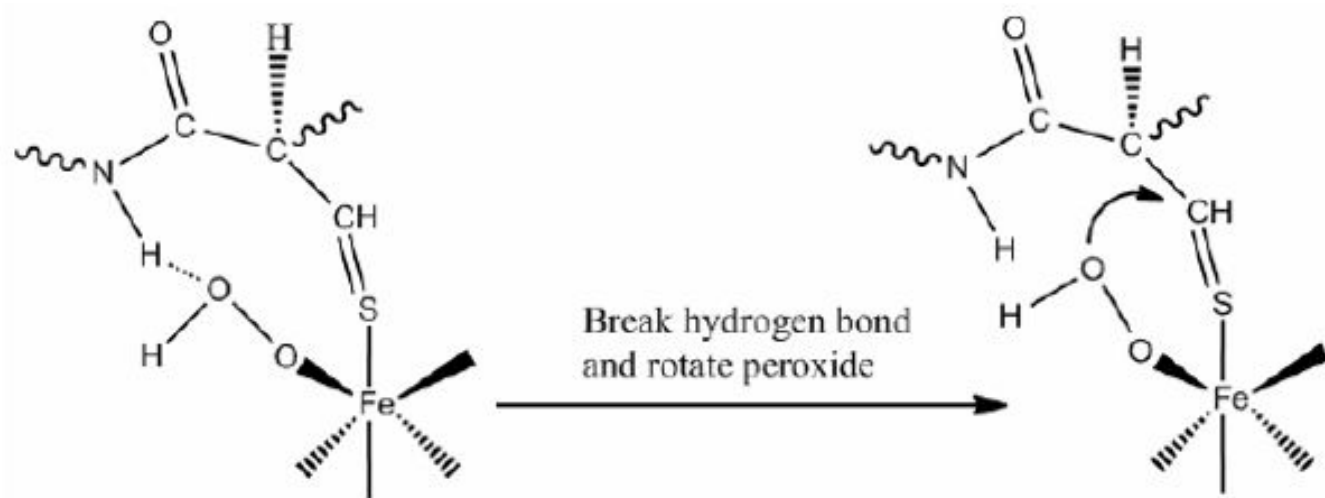
Deprotonation of the ACV amide leaves a lone pair on the amide N with the correct orientation for S_N2 nucleophilic attack at the C-S double bond.



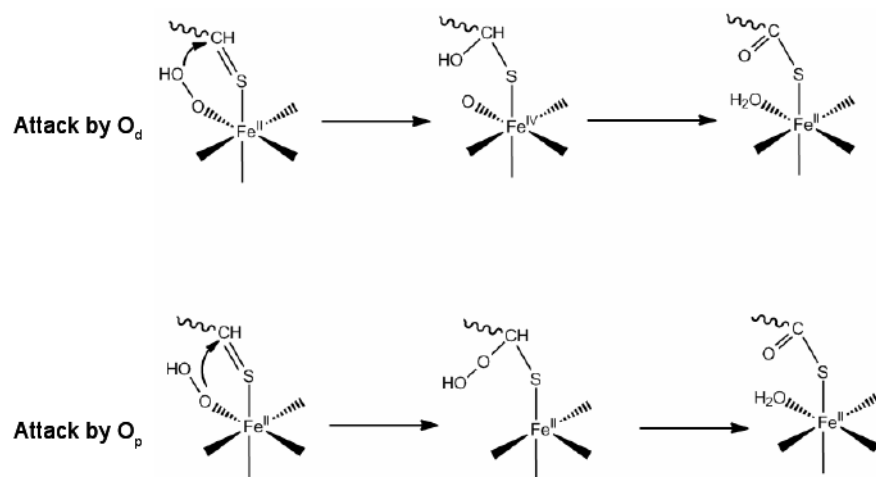
Scheme 1. The four electron oxidative double ring closure of ACV to form Isopenicillin N



Scheme 2. Three Reaction Pathways of Fe^{II}-Hydroperoxide



Scheme 3. Rotation of the Peroxide for Nucleophilic Attack



Scheme 4. Nucleophilic Attack by the distal and proximal oxygen of the hydroperoxide